Electronic structure of ferromagnetic iron: Band structure and optical properties

Tashi Nautiyal
Department of Physics, Lucknow University, Lucknow 226 007, Uttar Pradesh, India

Sushil Auluck
Department of Physics, University of Roorkee, Roorkee 247 667, Uttar Pradesh, India

(Received 30 September 1985)

A theoretical study of the band structure, density of states, and the optical properties of ferromagnetic iron is presented. The interpolation scheme parameters are those from our previous paper [Phys. Rev. B 32, 6424 (1985)]. The results are compared with other theoretical and experimental results. Upon comparing them with the recent angle-resolved photoemission data, we find the band structure to be fairly good. The resulting optical properties show a very good agreement with the experimental results.

I. INTRODUCTION

There are successful calculations of Fermi surface and optical properties of Cu,[1,2] Pd,[3] and Pt (Ref. 3) using the interpolation scheme. Ferromagnetic iron has d bands crossing the Fermi level and therefore has much more complicated band structure. We apply interpolation scheme to study the Fermi surface[4] and optical properties, in this paper, of ferromagnetic iron to check its validity in case of transition metals having complicated band structure. In our previous paper on ferromagnetic iron,[4] we developed a Fermi surface model and worked out a set of interpolation scheme parameters which yielded a sufficiently good estimation of the extremal orbit areas. We chose the interpolation scheme because it is fast and simple. Our results have the best agreement with the experimental Fermi surface as compared to other theoretical results.[4] We also focused our attention on the interference orbits which were otherwise untouched theoretically. Our results on the interference orbit areas were in agreement with the experimental results[5] though we are unable to obtain the fifth interference orbit (see Ref. 4), because the hole arms along HN get pinched off in our Fermi surface model. This does not seem to be very serious in view of the present ambiguity existing for the shape of the Fermi surface near symmetry point N in ferromagnetic iron.

While working out the problem of parametrizing the Fermi surface,[4] it becomes essential to keep in mind the energy band structure and related features, or else the fitted Fermi surface may result into a wholly absurd band structure. This is so because the Fermi surface, by its definition, is the locus of $\mathbf{k}$ points on a constant energy (E_F) surface. In this paper we study the band structure and optical properties of ferromagnetic iron. We are interested in finding out if our Fermi surface model[4] can yield a good representation for optical properties the evaluation of which involves band-level energies below as well as above Fermi energy. Availability of the experimental data for optical properties of ferromagnetic iron makes the task quite meaningful. Our calculations of optical properties involve the method of special directions for Brillouin zone integrations, hence our work is a good check of the accuracy of the special-direction method. We find that the calculations are in better agreement with the experiment as compared with other previous calculations in terms of peak positions and peak heights for the optical conductivity $\sigma_1(\omega)$.

II. RESULTS

A. Band structure

The energy eigenvalues we obtain are plotted along symmetry lines in Fig. 1. Table I presents the values at points of high symmetry. In a qualitative sense there is a general agreement in the overall shape of the bands with the other band calculations.[6-8] However, there is a striking difference between our calculations and those of Callaway and Wang[6] when the arrangement of energy bands at symmetry point N is considered. In our case, the level $N_1'(\uparrow)$ has an energy lower than the Fermi energy consequently, the hole arms (II) along HN direction[4] get pinched off whereas Callaway and Wang get an energy

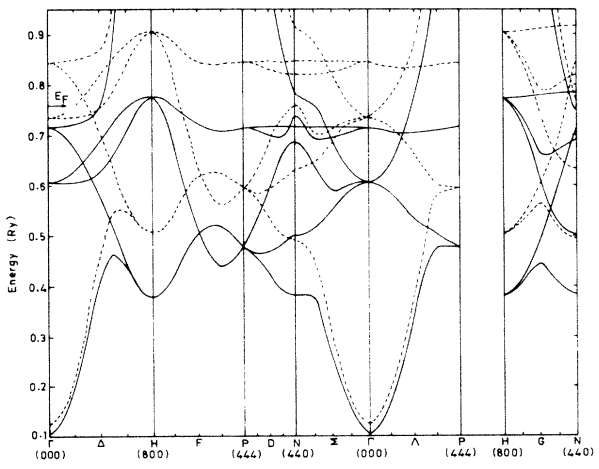

FIG. 1. Band structure of ferromagnetic iron. Solid (dashed) curves indicate majority (minority) spin bands.

TABLE I. Energy eigenvalues at the points of high symmetry. Values are in rydbergs.

Γ		H		P		N	
			(a) Spin-up electrons				
Γ_{12}	0.7134	H_{15}	1.4296	P_3	0.7143	N_3	0.7870
Γ_{12}	0.7126	H_{15}	1.4296	P_3	0.7143	N_1'	0.7416
Γ_{25}'	0.6050	H_{25}	0.7768	P_4	0.4819	N_4	0.7132
Γ_{25}'	0.6032	H_{25}	0.7751	P_4	0.4804	N_1	0.6903
Γ_{25}'	0.6015	H_{25}	0.7734	P_4	0.4789	N_2	0.5021
Γ_1	0.1061	H_{12}	0.3796			N_1	0.3852
		H_{12}	0.3796				
			(b) Spin-down electrons				
Γ_{12}	0.8437	H_{15}	1.4503	P_3	0.8443	N_3	0.9172
Γ_{12}	0.8436	H_{15}	1.4503	P_3	0.8442	N_4	0.8432
Γ_{25}'	0.7354	H_{25}	0.9069	P_4	0.5942	N_1	0.7623
Γ_{25}'	0.7333	H_{25}	0.9052	P_4	0.5942	N_1'	0.7623
Γ_{25}'	0.7326	H_{25}	0.9034	P_4	0.5926	N_2	0.6318
Γ_1	0.1208	H_{12}	0.5028			N_1	0.4950
		H_{12}	0.5028				

greater than Fermi energy E_F at $N_1'(\uparrow)$ and, therefore, extended hole arms (II) along HN. Also, our results show a considerable difference in energy eigenvalues at critical points N_1' and N_3 for spin up with N_1' having a lower energy than N_3. Wang and Callaway obtain nearly equal energy eigenvalues at $N_1'(\uparrow)$ and $N_3(\uparrow)$ with N_1' having a slightly higher value. We obtain an energy only slightly higher than E_F at $N_1'(\downarrow)$, consequently, a small orbit area for N centered VIII orbit[4] which is in far better agreement with the experimental orbit area[9] than that from Callaway and Wang[6] who obtain the energy at $N_1'(\downarrow)$ sufficiently larger than the Fermi energy.

For a comparison with experiment and other theoretical works, critical point binding energies are presented in Table II. The three data sets of Wang and Callaway have different origins. The first two sets have been obtained using local exchange potential with $\alpha=\frac{2}{3}$ [Kohn-Sham-Gaspar value (KSG)] and $\alpha=0.64$, an empirically chosen value, and the von Barth–Hedin (vBH) exchange-correlation potential has been employed for the third set. Our results for the binding energies seem to be in better agreement with the experiment[10] than the calculations from Jansen[7] and Moruzzi *et al.*[11] The band-level energy at critical points $\Gamma_{25}'(\uparrow)$, $\Gamma_{12}(\uparrow)$, $\Gamma_{25}'(\downarrow)$, $P_3(\uparrow)$, $N_1(\uparrow)$, $N_4(\uparrow)$, and $N_1(\downarrow)$, are in close agreement with the experiment.[10] One interesting feature that we observe is that even though the exchange parameters are constant,[4] the exchange splitting shows some anisotropy, e.g., the *sp* band originating from Γ_1 has a small exchange splitting but it exhibits a considerably large exchange splitting at

TABLE II. Critical-point band-level energies in eV measured from the Fermi energy.

	Expt.[a]	This work	KSG	Callaway[b] $\alpha=0.64$	vBH	Jansen[c]	Moruzzi[d]
$\langle\Gamma_{1\uparrow\downarrow}\rangle$	8.15±0.20	8.75	8.13	8.29	8.12	8.93	8.42
$\Gamma_{25}'\uparrow$	2.35±0.10	2.13	2.32	2.32	2.25	2.50	2.48
$\Gamma_{12}\uparrow$	0.78±0.10	0.64	0.94	0.92	0.84	1.44	0.97
$\Gamma_{25}'\downarrow$	0.27±0.05	0.36	0.02	0.15	0.43	0.45	0.45
$H_{12}\uparrow$	3.80±0.30	5.37	4.57	4.61	4.50	5.60	5.17
$H_{12}\downarrow$	2.50±0.30	3.50	2.71	2.87	2.99	3.43	3.71
$P_4\uparrow$	3.20±0.10	3.80	3.23	3.26	3.17	3.61	3.50
$P_3\uparrow$	0.60±0.08	0.62	0.73	0.71	0.53	1.77	0.68
$P_4\downarrow$	1.85±0.10	2.25	1.59	1.75	1.83	2.18	1.95
$N_1\uparrow$	4.50±0.23	5.10	4.80	4.86	4.75	5.52	5.24
$N_2\uparrow$	3.00±0.15	3.50	3.34	3.36	3.27	3.73	3.65
$N_1\uparrow$	0.70±0.08	0.75	0.94	0.92	0.86	1.25	0.94
$N_4\uparrow$	0.70±0.08	0.64	0.77	0.74	0.69	1.21	0.72
$N_1\downarrow$	3.60±0.20	3.60	3.40	3.57	3.60	4.18	3.92
$N_2\downarrow$	1.40±0.10	1.74	1.26	1.40	1.62	1.89	1.82

[a]Reference 10.
[b]Reference 6.
[c]Reference 7.
[d]Reference 11.

H, P, and N. This is due to the mixing or hybridization of different bands. The hybridization removes a number of band crossings. Most of the degeneracies are resolved by spin-orbit coupling. We have used the atomic value of spin-orbit coupling parameter.[12]

The exchange splitting in our model varies from 0.02 to 0.13 Ry. The splitting is small where the bands are predominantly *sp* like. A comparison of exchange splittings at various symmetry points with the experimental data[10] and other theoretical calculations[6,7,11] is presented in Table III. Our calculations are in good agreement with the experiment at H_{12}, P_4, and N_2. A slightly lower value is obtained at Γ'_{25}. It is interesting to note that our calculations give a better overall agreement with the experiment in comparison with other theoretical calculations. When compared to exchange splitting for Ni,[13] we find that E_s and E_d for Ni (0.005 and 0.032 Ry, respectively) are very small as compared to those for iron[4] (0.0207 and 0.130 Ry, respectively), which is indicative of stronger exchange interaction in ferromagnetic iron.

B. Density of states

We used the method of special directions[14] to perform the integrations over the Brillouin zone. For best results in terms of computer time and accuracy, 50 **k** points and 66 special directions were taken. In the earlier work[3] on Pt and Pd, 66 directions were found to be sufficient to get a good representation of density of states (DOS). The DOS for spin-up and spin-down electrons was separately calculated by neglecting spin-orbit coupling. The calculated DOS for spin-up and spin-down bands is shown in Figs. 2(a) and 2(b), respectively. From these figures we observe that the DOS curves for both types of bands are quite similar in nature although the width of the *d* band is slightly different for the two.

For the calculation of total DOS, we include the spin-orbit coupling. The total DOS, shown in Fig. 3, has two sharp peaks corresponding to the high DOS of *d* bands of the two spins in those regions of energy. The DOS for the ferromagnetic iron shows a sharp peak about 0.6 eV below the Fermi energy E_F which is in good agreement with the value of 0.58 eV estimated by Pessa *et al.*[15] from observations of their photoemission experiments, and with the calculation of Callaway and Wang.[6] We get a second peak in DOS 2.6 eV below E_F which is found to be

TABLE III. Exchange splitting at symmetry points. All values are in eV.

	Γ'_{25}	H_{12}	P_4	N_2
Experiment[a]	2.08±0.10	1.30±0.30	1.35±0.10	1.60±0.15
This work	1.77	1.67	1.28	1.76
Jansen[b]	2.05	2.17	1.43	1.84
vBH	1.82	1.51	1.34	1.65
Callaway[c] KSG	2.30	1.86	1.64	2.08
$\alpha=0.64$	2.17	1.74	1.51	1.96

[a]Reference 10.
[b]Reference 7.
[c]Reference 6.

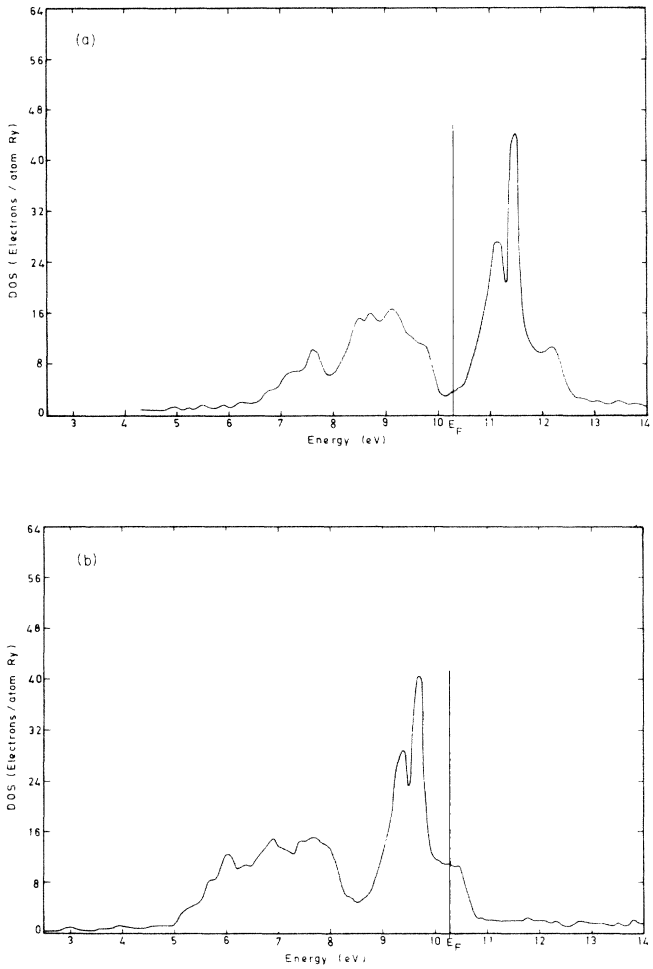

FIG. 2. (a) Density of states for spin-up (majority) electrons. Spin-orbit coupling has been neglected. (b) Same for spin-down (minority) electrons.

present at about 2.4 eV below E_F by experimentalists.[15–17] However, perhaps the agreement between our calculations and the experimental results may be improved by changing the parameters of the band structure slightly.

Our DOS curve displays small peaks at about 3.2 and 4.25 eV below E_F which may also be observed in other DOS calculations. We obtain another prominent peak at about 1.2 eV above E_F, thus a separation of about 1.8 eV between the two main peaks in the DOS. This separation between these two main peaks is representative of our exchange splitting parameter E_d (1.8 eV) between the *d* bands of opposite spins. Callaway and Wang[6] obtain this second peak at about 1.52 eV above E_F thus obtaining a larger value of E_d (2.18 eV). This peak is not observed in any of the experimental DOS since these are from photoemission measurements which give energy distribution of valence bands (i.e., occupied states) only.

Experimental studies by Blodgett and Spicer[16] reveal maxima in the valence-band optical DOS at 0.35, 2.4, and 5.5 eV below E_F. Two dominant peaks are resolved at 0.5 and 1.1 eV below E_F in the experimental work of East-

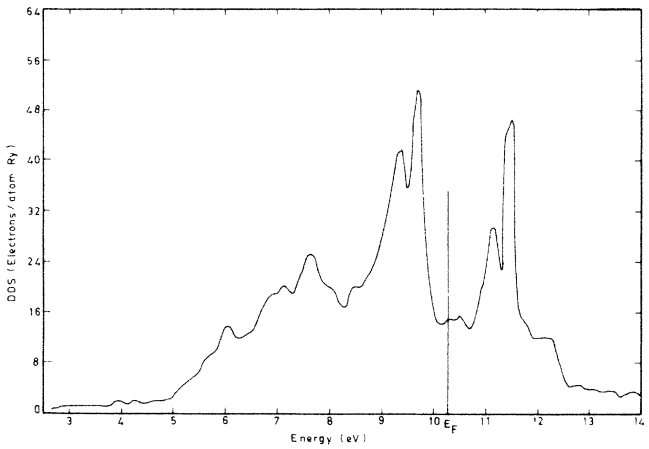

FIG. 3. Total density of states for ferromagnetic iron. Spin-orbit coupling taken into account.

man.[17] In our case these peaks are identified at 0.6 and 0.95 eV below E_F. A shoulder is experimentally resolved at 2.1 eV below E_F,[17] which is difficult to locate in our DOS as it has much more complicated structure around 2.1 eV below E_F than the experimental DOS. In the DOS measured by Eastman there is no peak at 5.5 eV below E_F which is present in the work of Blodgett and Spicer and it is attributed to surface contamination.[17] Our calculations do not show any such peak.

From the DOS for ferromagnetic iron the Fermi energy comes out to be 0.757 Ry which is in close agreement with the value 0.76 Ry set by us in the process of fitting the Fermi surface.[4] The value of Fermi energy, evaluated in this way, for ferromagnetic iron is lower than 0.77 Ry, the Fermi energy for paramagnetic iron.[18] This lowering in the Fermi energy may be the manifestation of the fact that the ground state of iron is stable in ferromagnetic configuration.

Our calculations give the magneton number

$$n_M = n\uparrow(E_F) - n\downarrow(E_F)$$

equal to 2.18 electrons/atom as compared to the experimental value of 2.12 electrons/atom.[19] Our method of calculating the magneton number may introduce an error, though quite small in magnitude, due to neglect of spin-orbit coupling during the computation of DOS of spin-up and spin-down bands.[20] This justifies, to some extent, the slight deviation of our n_M value from the experimental value.

The calculated value of the DOS $[N(E_F)]$ at the Fermi level is 14.658 states/Ry atom. The experimental value[21] of 27.37 is about twice as high. This indicates a large mass enhancement due to the interactions of electrons with phonons and magnons. The mass enhancement factor λ is defined as

$$\lambda = \frac{N_{\text{expt}}}{N_{\text{theor}}} - 1 ,$$

where subscripts expt and theor stand for experimental and theoretical values, respectively. The values of the magneton number, the DOS at Fermi level $[N(E_F)]$, the DOS of spin up $[N(E_F)\uparrow]$ and spin down $[n(E_F)\downarrow]$ electrons at the Fermi level, and the mass enhancement factor (λ) are presented in Table IV along with the values from other calculations and from experiments. Our results on n_M are in good agreement with the first-principles calcu-

TABLE IV. The magneton number n_M, density of states at the Fermi level $N(E_F)$ (in states/Ry atom), and enhancement factor λ ($=N_{\text{expt}}/N_{\text{theor}}-1$).

	Experiment	This work	Theory[a]	Theory[b]	Theory[c]	Theory[d]
n_M	2.12[e]	2.18	2.16	2.14	2.29	2.2
			2.30			
			2.35			
$N(E_F)\uparrow$		10.78	11.29			
			11.69			
			11.31			
$N(E_F)\downarrow$		3.71	3.35			
			3.68			
			3.10			
$N(E_F)$	27.37[f]	14.66	15.64	11.58	13.3	
			15.37			
			14.40			
λ		0.867	0.870	1.364	1.058	
			0.781			
			0.901			

[a]Reference 6.
[b]Reference 7.
[c]Reference 12.
[d]Reference 8.
[e]Reference 19.
[f]Reference 21.

lations of Callaway and Wang[6] and in fairly good agreement with other theoretical calculations.

C. Optical conductivity

Since the structure in $\sigma_1(\omega)$, the real part of the optical conductivity, is more prominent than that in $\epsilon_2(\omega)$, the imaginary part of the dielectric constant, and also since most of the calculations that have been reported are on $\sigma_1(\omega)$, we have decided to display our results on $\sigma_1(\omega)$ only. We study the interband contribution to $\sigma_1(\omega)$ which is related to $\epsilon_2(\omega)$ as

$$\sigma_1(\omega)=\frac{\omega\epsilon_2(\omega)}{4\pi} ,$$

where $\epsilon_2(\omega)$ is calculated using the general expression[22]

$$\epsilon(\omega)=\epsilon_1(\omega)+\epsilon_2(\omega)$$
$$=1+\frac{8\pi e^2}{3m^2}\sum_{i,f}\int_{\mathrm{BZ}}\frac{2d\mathbf{k}}{(2\pi)^3}\frac{|\hat{\mathbf{e}}\cdot\mathbf{M}_{fi}|^2}{(E_f-E_i)/\hbar}\times\left[\frac{(E_f-E_i)^2}{\hbar^2}-\left[\omega+\frac{i}{\tau}\right]^2\right]^{-1} ,$$

where the symbols have their usual meaning. The factor of $\frac{1}{3}$ in the above expression arises due to cubic symmetry of the crystal.[23]

We are required to calculate the momentum matrix elements of the form $\langle\psi_{fk}(\mathbf{r})|\nabla|\psi_{ik}(\mathbf{r})\rangle$ to evaluate $|\hat{\mathbf{e}}\cdot\mathbf{M}_{fi}|^2$. The usual procedure of band theory of taking the wave functions as Bloch functions has been adopted. Using the Ehrenfest's theorem,[24,25] the momentum operator may be written in terms of the Hamiltonian operator as

$$p(\mathbf{k})=\frac{m_0}{\hbar}\frac{\partial H(\mathbf{k})}{\partial k} .$$

In the interpolation scheme, since all the matrix elements of H are expressed as analytic functions of $\mathbf{k}$, the momentum matrix is, therefore, obtainable by a simple differentiation. The momentum matrix elements are thus directly expressed in terms of the specific band parameters and, of course, they are also $\mathbf{k}$-dependent. Here, we evaluate the matrix elements numerically for 66 special directions taking 50 $\mathbf{k}$ points along each direction. This would give us an accurate $\mathbf{k}$ dependence of the matrix elements. $\sigma_1(\omega)$ values from a band-structure calculation may be used as a means to estimate the accuracy of the underlying theoretical model. We compute $\sigma_1(\omega)$ under two situations. First, the collisionless case is taken up where the excited electrons are assumed not to relax by any mechanism (i.e., their relaxation time τ is infinite and relaxation energy $\hbar/\tau$ equal to zero). Next, we include the relaxation effects, a situation more close to reality since the excited electrons interact with the surroundings, hence relax due to interactions such as electron phonon and electron electron.

1. *Without relaxation effects*

Figure 4 presents result for $\sigma_1(\omega)$ when no relaxation of electrons is taken into account. Also shown are the $\sigma_1(\omega)$ values from the experimental data of Johnson and Christy[26] and Weaver *et al.*[27] The experimental data are shown on a larger scale in order to have the structures in it appear more clearly. Our calculations overestimate $\sigma_1(\omega)$ in most of the energy range.

Our $\sigma_1(\omega)$ curve depicts the main peak near 2.5 eV quite accurately. There is an overall agreement between our $\sigma_1(\omega)$ curve and the experimental ones. Our calculations show a faint hump around 5.5 eV which is seen in the form of a small peak at 6.1 eV in the experimental data[26,27] and also in the $\sigma_1(\omega)$ curve derived from the optical absorptivity data of Moravec *et al.*[28] We do not find any structure in the high-energy side. In the low-energy side, our curve shows change of slope, giving rise to small shoulders, near 0.5 and 1.1 eV. The dip around 1 eV in the total $\sigma_1(\omega)$ of ferromagnetic iron in the experimental data of Weaver *et al.*[27] is seen around 0.25 eV in our calculations of interband $\sigma_1(\omega)$. We do not expect this feature to match as the experimental data includes other contributions, such as the Drude term, owing to the intraband transitions within the conduction bands which are quite sizable at low energies.

2. *With relaxation effects*

The calculations of the interband contributions to the optical conductivity with the relaxation effects yield the results as shown in Fig. 5. Three values of relaxation energy $\hbar/\tau$, equal to 5, 10, and, 15 mRy, have been used of which only two (for $\hbar/\tau=5$ and 15 mRy) are shown in Fig. 5 for the sake of clarity. On comparing our $\sigma_1(\omega)$ with the experimental data, shown in the same figure, we find that the position of the main peak is reproduced quite accurately and the overall behavior of our $\sigma_1(\omega)$ resembles the experimental $\sigma_1(\omega)$,[27] except in the very-

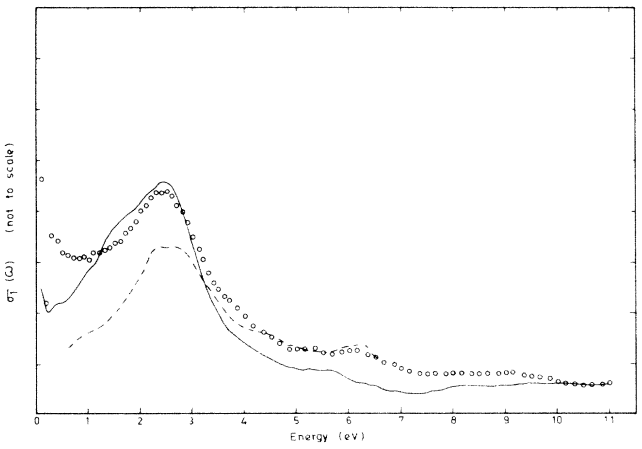

FIG. 4. $\sigma_1(\omega)$, the real part of optical conductivity, versus energy. Solid curve represents our results for collisionless case ($\hbar/\tau=0.0$ mRy). Circles and dashed-dotted curve represent experimental data of Refs. 27 and 26, respectively.

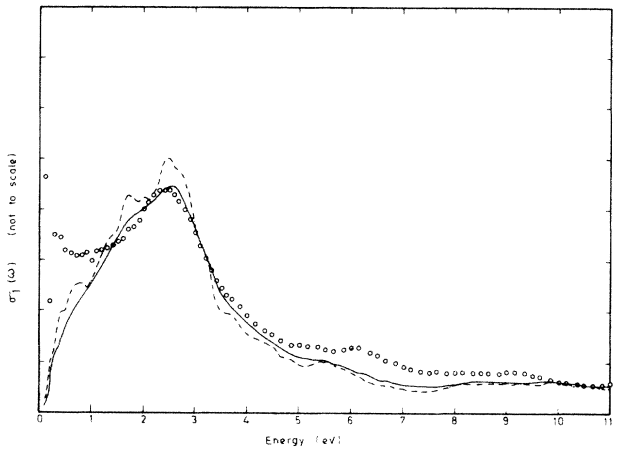

FIG. 5. $\sigma_1(\omega)$ with relaxation effects. Dashed (solid) curve represents theoretical results for $\hbar/\tau=5$ mRy (15 mRy). Circles have same meaning as in Fig. 4.

low-energy range below 1 eV, which is quite understandable for reasons cited in the preceding subsection. Once again[29] we observe that the higher the relaxation energy, the smoother the peak structure in $\sigma_1(\omega)$. We may very well predict that still higher values of relaxation energy may wash out all the structure in $\sigma_1(\omega)$ leaving a broad main peak. In this context the value of relaxation energy, equal to 0.3 eV (22 mRy), used by Singh *et al.*[12] is quite large.

Besides the main peak, the second peak which is comparatively mild and observed experimentally at 6.1 eV (Refs. 27 and 28) appears in our $\sigma_1(\omega)$ ($\hbar/\tau=5$ mRy) near 5.5 eV. This peak, being of very small strength, gets washed out when relaxation energy is taken as high as 15 mRy. The difference in the position of this peak in our $\sigma_1(\omega)$ and in the experimental $\sigma_1(\omega)$ seems to suggest some dissimilarity regarding the magnitudes of the energy gaps in the calculated and the actual band structure in this range (taking the experimental data to be true representative of actual situation). This peak is reproduced at a still farther position of 5 eV in the theoretical work of Singh *et al.*[12] The theoretical study of Laurent *et al.*[30] does show a peak and a shoulder near 6 eV, however, their calculations of interband $\sigma_1(\omega)$ yield this peak as prominent as the main peak. In the high-energy region, the slight hump in the experimental data near 9.2 eV is observable in our $\sigma_1(\omega)$ for relaxation energy equal to 5 mRy though the structure appears only faintly.

Our $\sigma_1(\omega)$ for 15 mRy case in the low-energy range shows change of slope near 1.7 eV, which is there in the experimental data also (Fig. 5). This feature appears as a small peak at 1.7 eV in the case of $\hbar/\tau$ equal to 5 mRy. We obtain another shoulderlike structure near 0.8 eV, which is also present in the work of Weaver *et al.*[31] The nature of decline in interband $\sigma_1(\omega)$ in this low-energy range agrees well with that from Weaver *et al.*[31] In all, we get better agreement with experimental $\sigma_1(\omega)$ as compared to other theoretical calculations.

For the interpretation of the structures in the optical conductivity of ferromagnetic iron, we assume that the mixing of the states with opposite spin due to spin-orbit coupling is small and that the spin-flip transitions do not contribute to the structures in the $\sigma_1(\omega)$. Most of the conductivity is expected to be due to transitions within the minority-spin band. The majority-spin bands are almost entirely occupied and would play an insignificant role in contributing to interband $\sigma_1(\omega)$.

The structure in $\sigma_1(\omega)$ near 0.8—1.0 eV arises mainly due to direct interband transitions near the N point among spin-up bands, while the structure at 1.7 eV may be attributed to direct transitions among spin-down bands near N and due to the transitions along $\Gamma(\Delta)H$ direction. The main peak near 2.55 eV has contribution from a large region among which the transitions at the N point, near the P point, and along the Δ axis are present. The transitions near H and N are responsible for the structure at 5.5 eV. The faint structure near 9.0 eV comes from transitions near the P and N points. Besides these transitions close to symmetry points, there appears to be a number of transitions along symmetry directions (Fig. 1) responsible for the structure in $\sigma_1(\omega)$. The structure near 0.3 eV in the $\sigma_1(\omega)$ appears to have contribution from the transitions in Σ direction near N point, and also from the transitions among spin-up bands near H along HN direction.

III. CONCLUSION

We find that our set of interpolation scheme parameters for ferromagnetic iron, which gives a good representation of the Fermi surface orbit areas and interference orbits,[4] is able to yield a good band structure and the density of states and a very satisfactory representation for the optical properties of ferromagnetic iron. The density of states we obtain is in reasonable agreement with the experimental results. The optical studies based on our band-structure parameters are quite encouraging. Though magnitude-wise our calculations overestimate the interband optical conductivity (real part), we find that our calculations of $\sigma_1(\omega)$ reproduce the structures and their positions very efficiently. From the comparison with the other theoretical studies on $\sigma_1(\omega)$ as well as with the experimental $\sigma_1(\omega)$, it is observed that our $\sigma_1(\omega)$ represents the structures in a better way than other calculations.

In summary, our band-structure model, even with the simple feature of constant exchange splitting, represents almost all the features of Fermi surface and optical properties of ferromagnetic iron in a satisfactory manner which is something quite encouraging to note.

ACKNOWLEDGMENTS

The financial support from University Grants Commission, India, is gratefully acknowledged. The authors are also thankful to the Roorkee University Regional Computer Center (RURCC) for providing the computer facilities.

[1]A. K. Ahuja, S. K. Joshi, and S. Auluck, Phys. Status Solidi B **118**, 575 (1983).
[2]A. K. Ahuja, Ph.D. thesis, University of Roorkee, India, 1982 (unpublished).
[3]A. K. Bordoloi, Ph.D. thesis, University of Roorkee, India, 1982 (unpublished).
[4]T. Nautiyal and S. Auluck, Phys. Rev. B **32**, 6424 (1985).
[5]R. V. Coleman, W. H. Lowrey, and J. A. Polo, Jr., Phys. Rev. B **23**, 2491 (1981).
[6]J. Callaway and C. S. Wang, Phys. Rev. B **16**, 2095 (1977).
[7]H. J. F. Jansen and F. M. Mueller, Phys. Rev. B **20**, 1426 (1979); H. J. F. Jansen, Ph.D. thesis, University of Groningen, The Netherlands, 1981 (unpublished).
[8]S. Wakoh and J. Yamashita, J. Phys. Soc. Jpn. **21**, 1712 (1966).
[9]G. G. Lonzarich, in *Electrons at the Fermi Surface*, edited by M. Springford (Cambridge University Press, Cambridge, 1980).
[10]A. M. Turner, A. W. Donoho, and J. L. Erskine, Phys. Rev. B **29**, 2986 (1984).
[11]V. L. Moruzzi, J. F. Janak, and A. R. Williams, *Calculated Electronic Properties of Metals* (Pergamon, New York, 1978).
[12]M. Singh, C. S. Wang, and J. Callaway, Phys. Rev. B **11**, 287 (1975).
[13]R. Prasad, S. K. Joshi, and S. Auluck, Phys. Rev. B **16**, 1765 (1977).
[14]R. Prasad and A. Bansil, Phys. Rev. B **21**, 496 (1980).
[15]M. Pessa, P. Heimann, and H. Neddermeyer, Phys. Rev. B **14**, 3488 (1976).
[16]A. J. Blodgett and W. E. Spicer, Phys. Rev. **158**, 514 (1967).
[17]D. E. Eastman, J. Appl. Phys. **40**, 1387 (1969).
[18]J. H. Wood, Phys. Rev. **126**, 517 (1962).
[19]H. Danan, A. Herr, and A. J. H. Meyer, J. Appl. Phys. **39**, 669 (1968).
[20]E. I. Zornberg, Phys. Rev. B **1**, 244 (1970).
[21]M. Dixon, F. E. Hoare, T. M. Holden, and D. E. Moody, Proc. R. Soc. London, Ser. A **285**, 561 (1965).
[22]R. W. Brodersen and M. S. Dresselhaus, in *Electron Density of States,* Natl. Bur. Stand. Spec. Publ. No. 323, edited by L. H. Bennett (U. S. GPO, Washington, D.C., 1971), pp. 39—45.
[23]A. O. E. Animalu, *Intermediate Quantum Theory of Crystalline Solids* (Prentice-Hall, Englewood Cliffs, 1977), p. 238.
[24]E. I. Blount, in *Solid State Physics,* edited by H. Ehrenreich, F. Seitz, and D. Turnbull (Academic, New York, 1962), Vol. **13**, p. 305.
[25]F. Szmulowicz and B. Segall, Phys. Rev. B **24**, 892 (1981).
[26]P. B. Johnson and R. W. Christy, Phys. Rev. B **9**, 5056 (1974).
[27]J. H. Weaver, C. Krafka, D. W. Lynch, and E. E. Koch, *Optical Properties of Metals* (Fach-informations-zentrum, Karlsruhe, Federal Republic of Germany, 1981), Pt. 1, pp. 75—87.
[28]T. J. Moravec, J. C. Rife, and R. N. Dexter, Phys. Rev. B **13**, 3297 (1976).
[29]T. Nautiyal and S. Auluck, J. Phys. F **18**, 2419 (1983).
[30]D. G. Laurent, J. Callaway, and C. S. Wang, Phys. Rev. B **20**, 1134 (1971).
[31]J. H. Weaver, E. Colavita, D. W. Lynch, and R. Rosei, Phys. Rev. B **19**, 3850 (1979).